AIAA 2002–2808

VALIDATION OF THE SIMULATION OF FLOW IN AN S-DUCT

R. D. D. Menzies, K. J. Badcock, G. N. Barakos, and B. E. Richards
CFD Group, Department of Aerospace Engineering, University of Glasgow, Scotland G12 8QQ, United Kingdom.

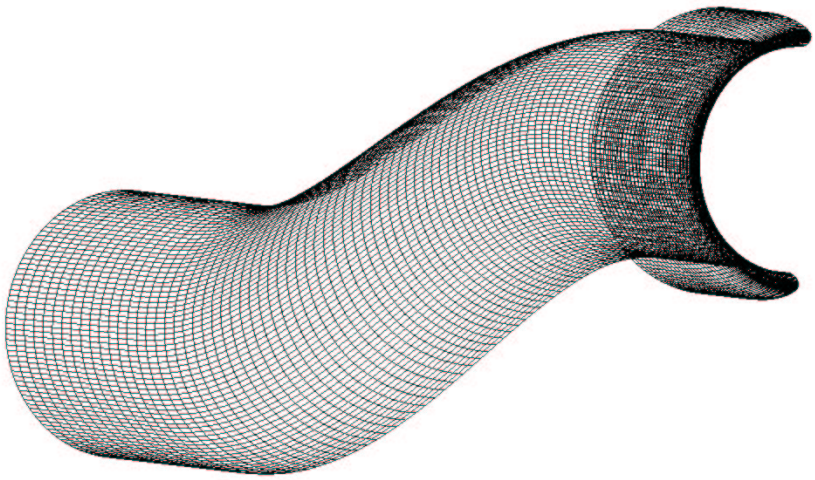

20th Applied Aerodynamics Conference
June 24–27, 2002/St. Louis, Missouri

VALIDATION OF THE SIMULATION OF FLOW IN AN S-DUCT

R. D. D. Menzies*, K. J. Badcock†, G. N. Barakos‡, and B. E. Richards§
CFD Group, Department of Aerospace Engineering,
University of Glasgow, Scotland G12 8QQ, United Kingdom.

Flow in a diffusing s-shaped intake has been examined using computational fluid dynamics simulations. This paper discusses the effects of different modelling techniques for such flows. Inviscid modelling gave a qualitatively good description of the flow for a simple low mass flow case. However it was seen that at high mass flow rates the inviscid solution is unsteady unless a modification is made to the duct geometry. Navier-Stokes calculations were performed for the same high and low mass flow cases using a variety of turbulence models. Results were much more favourable for both cases. It was found that different closure techniques and convergence levels had major differences in terms of the flow features predicted.

Introduction

Background

SINCE the invention of the first jet engine, intake aerodynamics has been an important field with most improvements arising from wind tunnel tests. Problems such as intake structural damage due to engine surge tended to only be detected after prototype testing and flying. Wind tunnel testing methods have improved drastically over this period and the understanding of some important characteristics of flows in complex integrated intake ducts has followed as a consequence. Over the same period computational methods of tackling such problems have also evolved considerably and, coupled with a rapid performance increase in computing power, increasingly more complex investigations have been attempted, adding to the understanding of intake flow physics.

Intakes are a crucial sub-component of an aircraft. The efficiency is crucial as it makes contributions to the performance and handling characteristics of the aircraft. The primary purpose of the device is to offer the compressor face a uniform stream of air at specific conditions required by the engine whilst maximising efficiency and minimising total pressure loss.

Integrating an intake into an aircraft structure can often be challenging. Undercarriage wells and intake store bays often have to be negotiated leading to offset intake ducts. Intakes are also offset to provide low observability characteristics and reduce the radar cross section (RCS) of the aircraft as a large contribution to the RCS of an aircraft comes from the reflections of radar signals off the engine compressor face.

The flow in the RAE intake model 2129 (M2129) is complex. The flow accelerates into the intake from a stagnation point on the outer cowl surface. There is further acceleration of the flow around the starboard side first bend of the intake - Fig. 1 - where separation occurs. The faster moving core stream is acted upon by centrifugal and pressure forces which cause it to move towards the outside of the bend (port side). Here the flow meets an adverse pressure gradient. Energy deficient near wall fluid approaches this adverse pressure gradient but cannot pass through it. Instead the flow moves around the outside curve of the wall towards the lower static pressure on starboard side. This action of the low energy region towards the inside bend combined with the movement of the core flow towards the outside bend sets up two cells of contra-rotating secondary flow.

A consequence of the rotating flow can be an increase or decrease in the flow angle of attack on the compressor blades which can then lead on to stall. If a sufficient number of compressor blades stall then it is possible that an engine may surge which is an undesirable occurrence. Variations in flow angle of attack at the compressor face also cause a maldistribution of pressure which is quantified by a parameter called distortion. This parameter is usually given for a 60° sector that is worst effected.

*Research Student, corresponding author.
†Senior Lecturer.
‡Lecturer.
§Mechan Professor, AIAA Associate Fellow.

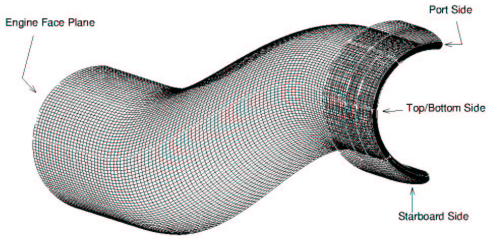

Fig. 1 M2129 intake geometry showing surface grid and intake definitions.

Test Case	M	PR	MFR	CR
1	0.21	0.9897	1.457	0.931146
2	0.21	0.9280	2.173	0.931146

Table 1 Summary of Test Case Conditions

Test Case

The two test cases that are examined here have been examined previously.[1] Test case 1 features a low mass flow rate and is relatively straightforward. The second case is more complex as it is for a high mass flow rate which is sufficient to develop supersonic flow within the intake.

The test case conditions can be seen in table 1. The contraction ratio (CR) is defined as the ratio of the area of the highlight plane to the area of the engine face plane, where the highlight plane is defined as the plane that cuts the leading edge of the cowl. The mass flow rate (MFR) can be thought of as being related to the engine demand. In physical terms, it is defined by the dividing streamline, the streamline that borders flow that enters the intake with flow that does not. It is the ratio of the dividing streamline in the freestream to the area of the highlight. For subsonic intakes the MFR is greater than 1. However, when considering supersonic flows, the MFR is less than one as the intake draws air from an area less than it's highlight area. The pressure recovery (PR) is a value estimated from experimental experience. Clearly a value as close to unity as possible is desirable.

These values can be used to determine a static pressure that is applied across the downstream plane. A constant static pressure boundary condition has been found to be suitable for strictly subsonic flows.[2] The boundary condition does not model the fan in any way, but only the engine demand. Setting the correct engine demand (applying the correct static pressure) is sufficient to model the upstream effects. This is a simplification in that the fan may impose a small amount of bulk swirl into the main flow but this has been found to be negligible. The downstream boundary has been placed far enough from the engine face to make all approximations valid.

Previous Work

Experimental and computational work have been published previously.[1,3–7] The first two references also consider the inviscid case. It was found from experiments that considerable secondary flow is a feature of the high mass flow case and so it is much more challenging. There are greater variations in results between experiment and computation for the high mass flow case. Inviscid results require an addition to the geometry to account for any displacement (separation) of the flow from the starboard side of the duct at the first bend.

Turbulent computational results in previous works did not require any modifications to the geometry. However there is also little information on convergence for the turbulent results. Indeed May[4] describes a failure to reach fully converged results. A reasonable qualitative comparison between experiment and computation for the low mass flow case was found for all previous computational works. Quantitatively, however, the comparison is not so good. Inviscid results overpredict key features and turbulent results fail to capture secondary flow satisfactorily. Overall it can be said that the variations in results between experiment and computation is considerable for the Euler calculations, even with modifications to the geometry. Turbulent results improve the predictions although convergence details are limited and secondary flow prediction is challenging. This paper aims to clarify the various problems associated with predicting inviscid and turbulent flows for these cases.

Simulation Method

The problem was modelled including the intake cowl and a large far field freestream region. This enabled the flow to be simulated from freestream into the duct and eliminated the need for complicated inflow boundary conditions to be developed. A further advantage is that a direct comparison between flow solvers is possible. For Navier-Stokes calculations, the flow was assumed to be turbulent in all but the freestream blocks and a symmetry boundary condition was implemented through the $x - z$ plane to reduce computational costs.

PMB,[8] Glasgow University's three-dimensional and two-dimensional flow solver, was applied to the problem. A cell centred finite volume technique is used to solve the Euler and Reynolds averaged Navier-Stokes (RANS) equations. The diffusive terms are discretised using a central differencing scheme and the convective terms use Roe's scheme with MUSCL interpolation offering third order accuracy. Steady flow calculations proceed in two parts, initially running an explicit scheme to smooth out the flow then switching to an implicit algorithm to obtain rapid convergence. The pre-conditioning is based on Block Incomplete Lower-Upper (BILU) factorisation and is also decoupled between blocks to improve parallel performance. The linear system arising at each implicit step is solved using a Generalised Conjugate Gradient (GCG) method.

The flow solvers have previously been applied to a wide range of problems including:

- Hypersonic spiked body flows[9]
- Rolling, pitching and more recently yawing delta wings[10]
- Two and three-dimensional cavity flows[11]
- Other complex three dimensional geometries

To study complex, inviscid, and more especially turbulent, 3D intake flows requires considerable computing power. The Computational Fluid Dynamics group at the University of Glasgow owns a clusters of PC's consisting of 32 nodes of 750MHz AMD Athlon Thunderbird uni-processor machines with 768Mb of 100MHz DRAM. A typical grid size of 500,000 points requires around 4 hours to complete 2000 implicit steady state steps at a CFL of 30 in order for the log of the residuals to drop 8 orders, at which point it is considered fully converged.

An aim of this paper is to assess the performance of various turbulence closures in modelling complex internal flows. The flow is challenging with complex secondary flows and strong adverse pressure gradients, generated by localised accelerating flows, placing high demands on turbulence models. Turbulence modelling is one of the central problems and remains a huge challenge in CFD.

The non-linearity of the Navier-Stokes equations has the effect of developing momentum fluxes (unknown a priori) that act as apparent stresses in the flow. Equations are developed for these stresses and include additional unknowns. It can be said that the function of turbulence modelling is to devise approximations for the unknown correlations in terms of flow properties that are known so that a sufficient number of equations exist. In making such approximations, we close the system.

Past research in relation to steady and unsteady turbulent flow simulations in the context of Reynolds Averaged Navier-Stokes (RANS), has shown that the realism of numerical predictions is significantly affected by the accuracy of the turbulence model employed. Experience using zero-equation turbulence models (e.g. Baldwin and Lomax[12]) has shown that these models do not provide satisfactory results, especially in separated flows and their predictions depend upon empirical constants and topographic parameters which are case specific.

Linear eddy-viscosity models (LEVM) assume an explicit algebraic relationship between Reynolds stresses and mean strain, known as Boussinesq approximation (the principal axes of the Reynolds stress tensor (τ_{ij}) is computed as the product of the eddy viscosity (μ_T) and the mean strain rate-rate tensor (S_{ij})). These models provide satisfactory results for attached, fully developed turbulent boundary layers with weak pressure gradients and are also relatively easy to implement into computational fluid dynamics (CFD) codes. However, the predictions deteriorate when all components of the Reynolds-stress tensor become dynamically significant.

Linear low-Re two-equation models seem to offer the best balance between accuracy and computational cost, but since they employ the Boussinesq approximation for the Reynolds stress tensor, are not able to capture effects arising from normal-stress anisotropy. Second-moment closures offer a more exact representation of the Reynolds stresses but require longer computing times and careful numerical implementation for obtaining stable numerical solutions. Reynolds-stress models have been used in the past to investigate shock/boundary layer interaction (see Davidson 1995;[13] Batten et al,[14] amongst others). These studies showed that in certain cases second-moment closures may provide better results than linear models, but in other cases the results are inconclusive. Other approaches in turbulence modelling include the non-linear eddy viscosity models (NLEVM) (Speziale;[15] Craft et al[16]) and explicit algebraic stress models (see Gatski;[17] Abid et al[18,19]).

NLEVM's is one of the approaches employed in this study. The objective of this approach is to introduce closures that incorporate key fea-

tures of the Reynolds-stress models, but which, however, require computational effort comparable to linear two-equation eddy-viscosity models. The idea behind non-linear eddy-viscosity models can be found in the paper of Pope,[20] while later on Speziale[15] and Speziale and Ngo[21] demonstrated the ability of non-linear models to capture secondary flows in ducts and flows over backward-facing steps, respectively. Furthermore, Rubinstein and Barton[22] developed a non-linear model based on the re-normalisation group theory (Yakhot and Orszag;[23] Orszag[24]), while Shih et al[25] developed a realisable non-linear algebraic-stress model.

A different approach was taken by Apsley and Leschziner[26] who developed a low-Re NLEVM by simplifying a second-moment closure. Other attempts to use advanced turbulence models in aerodynamic flows can be found in the works by Gatski,[17] Jiang et al,[27] amongst others. The experience from steady flows has shown that NLEVM's offer some promising capabilities in terms of accuracy and, additionally, are more economic in terms of computing resources compared to the Reynolds-stress transport models. Non-linear models have been and are still being refined and validated for steady flows, mainly two-dimensional and incompressible (see Craft et al[16,28]), while limited experience has been acquired from applications to compressible flows (e.g. Gatski[17] and Barakos and Drikakis[29]). Although most of the NLEVM's have emerged from the $k-\epsilon$ EVM, efforts have also been made to develop a $k-\omega$ NLEVM.[30]

This paper has employed the S-A model,[31] $k-\omega$,[32] and it's hybrid, the SST model.[33] These models are eddy viscosity models. One-equation models have perhaps been the least successful and used of all the models devised. The S-A falls into this category and has been used for this work. It was chosen as it gives improved prediction of flows with adverse pressure gradients compared with the $k-\omega$ or $k-\epsilon$ models.

The $k-\omega$ turbulence model is a two-equation model and is also based on the Boussinesq eddy viscosity hypothesis. The eddy viscosity coefficient is determined from the solution to two partial differential equations - one for the turbulent kinetic energy (k) and one for the specific dissipation rate (ω). The rate of dissipation of energy in unit volume and time is related to the external scale of turbulence, l. Consequently such 2 equation models are termed as complete as they can be used to predict turbulent flow without initial knowledge of the turbulent flow structure.

The SST turbulence closure technique is a two-equation model that is a hybrid of the $k-\omega$ and $k-\epsilon$ models. Closures that are Boussinesq-like are notoriously unreliable for flows with secondary motions. The eddy viscosity formulation is modified to account for transport effects of the principal turbulent shear stress by forcing the turbulent shear stress to be bounded by a constant times the turbulent kinetic energy inside the boundary layer (a realisability constraint). By doing this, the modification improves the prediction for flows that have separation and are dominated by strong adverse pressure gradients. To this end, it was expected that SST predictions would show improvements over standard $k-\omega$ and one-equation $S-A$ predictions for flows in diffusing offset internal ducts.

Examination of Results

Low Mass Flow Rate

As mentioned, the low mass flow rate case is considered the easier of the two test cases. Flow acceleration into the intake duct is subsonic at all times and secondary flow generation is not so intense relative to the high mass flow case. This brings problems in terms of turbulence modelling as it has been proven difficult[1,5] to predict secondary flow satisfactorily using computational techniques.

Inviscid

Fully converged results were obtained for the Euler calculation. Figure 2 shows the ratio of the local static pressure to freestream total pressure from the starboard surface of the duct. There is a significant over-prediction in the flow acceleration into the intake. This has knock-on effects as the pressure does not recover and drops again at the first intake bend ($X/D=1$) on the starboard side by around 10% more than witnessed in the experiments. There is no inviscid separation off of the first bend and secondary flow is, of course, not predicted.

Turbulent

Various closure techniques were used for the turbulent calculations. Fully converged solutions were reached in all cases, fully converged meaning the residuals had dropped 8 orders of magnitude. Figure 2 shows the pressure trace from the starboard side of the duct for all models compared against previous computation and experiment.[1] Flow acceleration around the cowl is well predicted for all models. The subsequent pressure recovery is over-predicted for the SST and SA. The $k-\omega$ model shows a very close match with experiment upstream of the first bend.

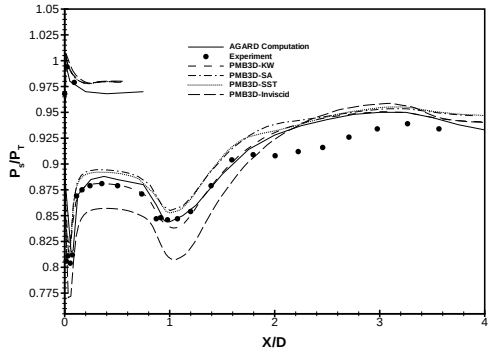

Fig. 2 LMFR, turbulent. Pressure extraction's from the starboard side of the intake.

It has been documented previously[1,3,4] that the prediction of secondary flow for this case has been challenging. Secondary flow can be detected by a dip in the static pressure trace downstream of the first bend as witnessed for the experimental data. Close examination of the figure suggests that all models fail to predict any significant secondary flow.

However the graph shows that the SST model does show signs of dipping. The magnitude of this drop is not sufficient to match experimental data. However it can be seen that the pressure recovery in the cowl region is greater than witnessed in experiment and this leads to a higher pressure from the first bend downstream. Figure 3 shows a contour plot of the ratio of local to freestream total pressure at the engine face plane on one half, with velocity vectors plotted in the second half. Lower total pressures are seen due to the secondary flow and this is highlighted by the vector plot showing a small swirling vortex.

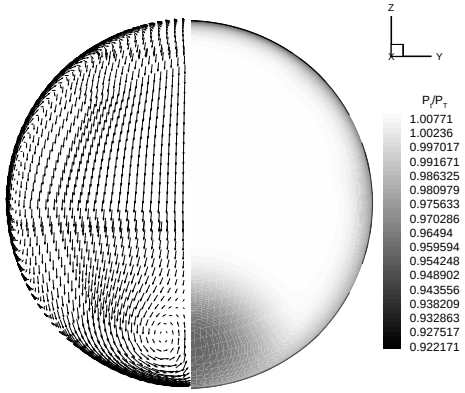

Fig. 3 LMFR, SST model. Secondary flow at the engine face.

The $k-\omega$ predictions match the previous AGARD computation and experimental data closely throughout the cowl and to the first bend. Following the first bend the result deviates with the computations remaining closely matched and deviating from the experimental data which shows stronger secondary flow. The SA results are closer matched to the SST results in the cowl region. Following the first bend the separation predicted is less leading to a poorer simulation of secondary flow.

High Mass Flow Rate

The high mass flow case is known to be challenging. The engine demand is such that supersonic flow is generated at the cowl as the flow accelerates into the duct, but also on the starboard side at the first bend. Again inviscid and turbulent calculations have been performed.

Inviscid

A converged solution for the Euler calculation was not found. The issue of the convergence problem is likely to be from one of two sources: the problem as modelled is not steady, or the domain boundary conditions are unrealistic. The unsteady flow solver was run. The pressure history is plotted in Fig. 4 from a point on the centreline at the first bend. It is evident that the pressure is fluctuating by around $\pm 15\%$ about the mean value and is periodic. Further analysis revealed that the problem exhibits inviscid separation off of the starboard side first bend, this being the contributing source of the unsteadiness. The literature is limited with regard to the high mass flow inviscid case. However there is a description of a case where a modification reference is made to the geometry that accounts for any 'displacement' of the flow.[3] It is thought that such a modification would solve the problem of unsteadiness experienced although time constraints did not allow this to be verified. The more salient problem was that of turbulence modelling and so attention focused on that.

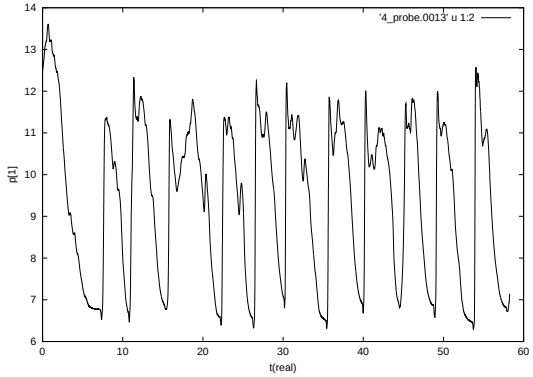

Fig. 4 HMFR, inviscid. Pressure time history from a probe on the centreline at the first bend.

Turbulent

Figure 5 shows pressure extraction from the starboard side from all models examined. Once again the results are compared against experiment and previous computational solutions (using the $k-\omega$ model). It is clear that there are major problems with the results for the SA and $k-\omega$ models from PMB. Flow acceleration into the duct is over-predicted. This appears to lead to a complex shock reflection system in the cowl region, more especially for the $k-\omega$ results. The SA results recover somewhat prior to the first bend.

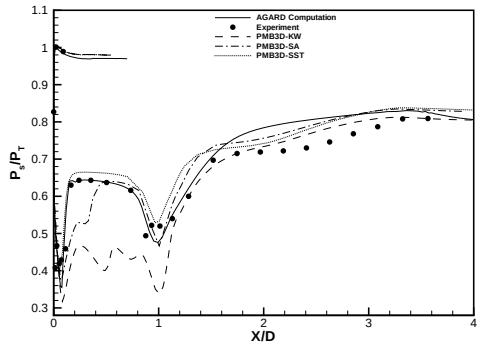

Fig. 5 HMFR, turbulent. Pressure extraction's from the starboard side of the intake.

All models predict significant secondary flow. The $k-\omega$ results give the closest match with experiment but this is primarily due to the pressure recovery problems in the cowl. Consequently it is the SST results that are again the most satisfactory. Figures 6 and 7 show contours of total pressure and velocity vectors at the engine face, and total pressure at locations through the duct. The extent of the maldistribution of pressure across the engine face is evident.

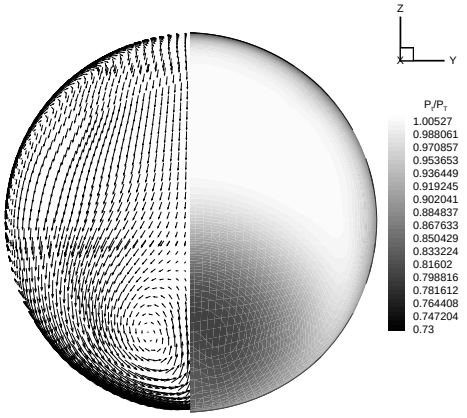

Fig. 6 HMFR, SST. Secondary flow at the engine face.

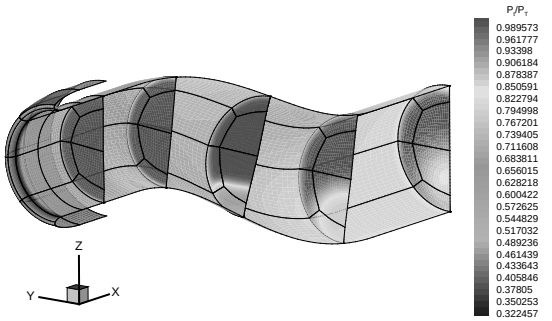

Fig. 7 HMFR, SST. Secondary flow at locations through the intake.

Figure 8 shows the interior surface of the intake with streamlines of shear stress. As the flow approaches the first intake bend flow on the upper port side is swept round the curvature of the bend by the mechanisms described in the introduction. As one moves round the surface of the intake from the port to the starboard sides, a point is reached where the flow spirals to a saddle point.

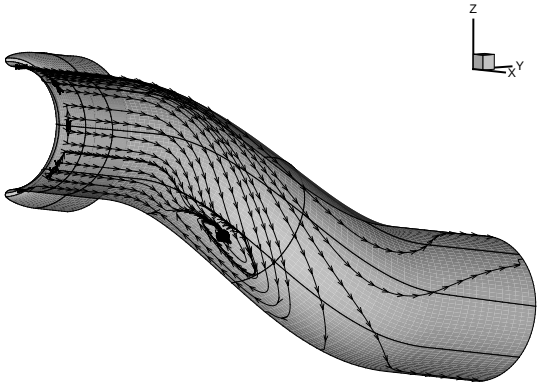

Fig. 8 HMFR, SST. Surface shear stress showing spiral node and saddle point.

The boundary layer profile through the starboard side following the flows acceleration into the duct is shown in Fig. 9. The graph shows the u-velocity non-dimensionalised with freestream velocity plotted against distance from the wall. The $k-\omega$ and $S-A$ models have very similar profiles and vary from the profile obtained with the $S-A$ model. The $S-A$ model shows a much lower velocity as you move away from the

wall surface. There is also a small pocket of separation that can be seen in the graph as a negative component of u-velocity. Both the $k-\omega$ and $S-A$ models do not predict this small separated region in the cowl flow. It can also be seen that peak velocities actually occur closer to the wall, not in the core as may be thought, due to the large acceleration of the flow around the cowl and into the duct.

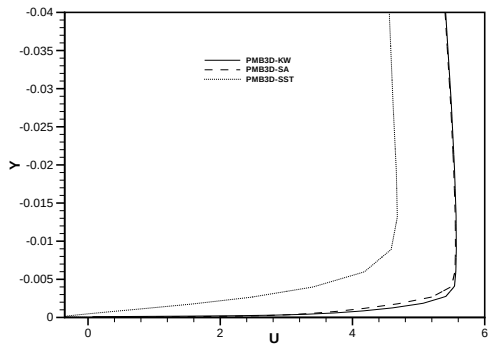

Fig. 9 HMFR, turbulent. Extraction of the u-velocity through the boundary layer.

In studying the literature on previous computational work on this problem, it is hard to find clear information on the level of convergence achieved in other calculations. As mentioned, all calculations here are considered fully converged when the log of the residuals reduces 8 orders of magnitude. However there is previous work that states that some computations are considered fully converged when the residuals are reduced 4 orders.[1] For comparison, all turbulence closure techniques were re-run and stopped when the residuals had dropped 4 orders.

Figure 10 shows the pressure history through the duct from the starboard side for this reduced convergence case. Comparison with fully converged results in Fig. 5 shows some major differences. Initial flow acceleration into the duct is now better predicted for all models. The subsequent pressure recovery is over-predicted for although the $k-\omega$ model is promising. However this model greatly over-predicts the starboard acceleration around the first bend. There follows a strong local shock which leads to a good agreement with the other models downstream of the first bend. The $S-A$ and SST models predict a greater pressure recovery in the cowl region than was seen in experiment. However these models better predict the starboard side acceleration at the first bend. Secondary flow is predicted with all the models but the characteristic dip or saddle in the pressures trace between the two bends is not evident.

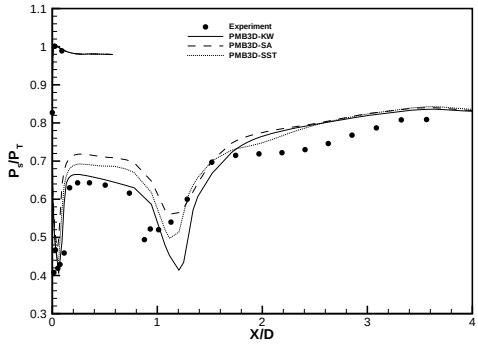

Fig. 10 HMFR, turbulent. Pressure extraction's from the starboard side of the intake for solutions converged 4 orders of magnitude.

Conclusions

Euler and Reynolds-averaged Navier-Stokes equations (using various closure techniques) has been applied to the problem of predicting flow in the RAE intake model 2129, an offset diffusing s-shaped aircraft intake. The aim was to clarify the effects of different modelling techniques for a standard low and high mass flow case.

Euler calculations for the low mass flow case were qualitatively good. However flow acceleration into the duct was over-predicted and secondary flow was obviously not captured leading to a poorer comparison of the pressure levels through the duct. The high mass flow case was found to be unsteady with the origins of this coming from flow separation off the starboard side first bend. The literature revealed that this case had not been as widely studied and that previous work had made modifications to the geometry to account for any displacement of the flow from the starboard side first bend.

Turbulent calculations for the low mass flow case were much more promising. Comparison with experiment and previous computation was better. The prediction of secondary flow for this case is known to be challenging. It was found that all models predicted limited secondary flow, the SST model showing the strongest effects, although the pressure levels were around 6% higher.

The turbulent high mass flow case is complex. Secondary flow is better predicted for all models with the SST model again performing the best and comparing well with previous computation and experiment. The main problem was the prediction of the flow in the cowl region. The $k-\omega$ and SA models predicted complex shock

reflection in this region that was no found in experimental data. Previous computational work for this case does not discuss convergence in any detail although one reference mentions a drop in the residuals of 4 orders being fully converged. As this work considers fully converged to be a drop of 8 orders, calculations were re-run stopping at 4 orders. It was found that the solutions varied remarkably. The problem of shock reflection in the cowl is no longer present for the $k-\omega$ and SA simulations and the results show a much closer match for those models.

Acknowledgements

This work is supported by a Scholarship from the Defence Evaluation and Research Agency (DERA), Bedford.

References

[1]Fluid Dynamics Panel - Working Group 13. 1991 Test Case 3 - Subsonic/Transonic Circular Intake. *AGARD Advisory Report 270*.

[2]Chung J. and Cole, G. L. 1995 Comparison of Compressor Face Boundary Conditions for Unsteady CFD Simulations. *AIAA Paper 95-3590*.

[3]May, N. E., C.J.Peace, C.J. and McHugh, C. A. 1993 An Investigation of Two Intake/S-Bend Diffuser Geometries Using the Sauna CFD System - Phase 1. *ARA Memo 386*.

[4]May, N. E. 1995 The Prediction of Intake/S-Bend Diffuser Flow Using the Sauna CFD System with Two-Equation Turbulence Models. *ARA Contractor Report* **M268/5**

[5]May, N. E.1997 1997 *The Prediction of Intake/S-Bend Diffuser Flow Using Various Two-Equation Turbulence Model Variants, Including Non-Linear Eddy Viscosity Formulations. ARA Contractor Report* **M316/1**.

[6]Anderson, B. H., Reddy, D. R. and Kapoor, K. 1993 A Comparative Study of Full Navier-Stokes and Reduced Navier-Stokes Analyses for Separating Flows Within a Diffusing Inlet S-Duct. *AIAA Paper 93-2154*.

[7]Abrahamsen, P. E. H., Pettersson Reif, B. A., Saetran, L. and Fossdal, J B. 1998 Air Intake Studies: Experimental Measurements and Computational Modelling. Presented at*RTO AVT Symposium on "Missile Aerodynamics", Soreento, Italy, 11-14 May 1998, and published in RTO MP-5*.

[8]Badcock, K. J., Richards, B. E. and Woodgate, M. A. 2000 Elements of Computational Fluid Dynamics on Block Structured Grids Using Implicit Flow Solvers. *Progress in Aerospace Sciences*, **36**, 351–392.

[9]Feszty, D., Badcock, K.J. and Richards, B.E. 2000 Numerical Simulation of the Hysteresis Phenomenon in High Speed Spiked Body Flows. *AIAA Paper 2000-0141*.

[10]Arthur, M. T., Brandsma, F., Ceresola, N. and Kordulla, W. 1999 Time accurate Euler calculations of vortical flow on a delta wing in pitching motion *AIAA Paper AIAA 99-3110*.

[11]Henderson, J., Badcock, K.J. and Richards, B.E. 2000 Understanding Subsonic and Transonic Open Cavity Flows and Suppression of cavity tones *AIAA Paper 2000-0658*.

[12]Baldwin, B.S. and Lomax, H. 1978 Thin Layer Approximation and Algebraic Model for Separated Turbulent Flows. *AIAA Paper 78-257*.

[13]Davidson, L. 1995 Reynolds Stress Transport Modelling of Shock-Induced Separated Flow. *Computers and Fluids* **24**(3), 253-268.

[14]Batten, P., Craft, T. J., Leschziner, M. A. and Loyau, H. 1999 Reynolds-stress-transport Modeling for Compressible Aerodynamics Applications. *AIAA J.* **37**(7), 785-797.

[15]Speziale, C.G. 1987 On Non-linear $K-l$ and $K-\epsilon$ Models of Turbulence. *J. Fluid Mechanics* **178**, 459-475.

[16]Craft, T.J., Launder, B. E. and Suga, K. 1996 Development and Application of a Cubic Eddy-Viscosity Model of Turbulence. *International Journal of Heat and Fluid Flow*, **17**(2), 108-115.

[17]Gatski, T.R. 1996 Prediction of Airfoil Characteristics with High Order Turbulence Models. *Technical Memorandum 110246*. NASA.

[18]Aabid, R., Rumsey, C. and Gatski, T. 1995 Prediction of Non-equilibrium Turbulent Flows with Explicit Algebraic Stress models. *AIAA J.* **33**(11), 2026-2031.

[19]Aabid, R., Morrison, J.H., Gatski, T.B. & Speziale, C.G. 1996 Prediction of Aerodynamic Flows with a New Explicit Algebraic Stress Model. *AIAA J.* **34**(12), 2632-2635.

[20]Pope, S.B. 1975 A More General Effective Viscosity Hypothesis. *J. Fluid Mech.* **72**, Part 2, 331-340.

[21]Speziale, C.G. and Ngo, T. 1988 Numerical Solution of Turbulent Flow Past a Backward-Facing Step Using a Non-linear $k-\epsilon$ Model. *Int. J. Eng. Sci.* **26**, 1099-1112.

[22]Rubinstein, R. and Barton, J.M. 1990 Nonlinear Reynolds Stress Models and the Re-normalization Group. *Phys. of Fluids* **2**(8), 1472-1476.

[23]YakhotT, V. and Oorszag, S.A. 1986 Renormalization Group Analysis of Turbulence: I. Basic Theory. *J. Sci. Computing* **1**(1), 3-51.

[24]Orszag, S.A., Yakhot, V., Flannery, W.S and Boysan, F. 1993 Re-normalization Group Modelling and Turbulence Simulations. In *Near Wall Turbulent Flows* (ed. R.M. So & C.G. Speziale), pp. 155-183. Elsevier.

[25]Shih, T.-H., Zhu, J. & Lumley, J.L. 1993 A Realizable Reynolds Stress Algebraic Equation Model. *Technical Memorandum 105993*. NASA.

[26]Apsley, D.D. and Leschziner, A. 1997 A New Low-Re Non-Linear Two-Equation Turbulence Model for Complex Flows. *Eleventh Symposium on Turbulent Shear Flows, TSF-11*, pp 6-25–6-30.

[27]Jiang, Y.T., Damodaran, M. and Lee, K.H. 1997 High-resolution Finite Volume Computation of Turbulent Transonic Flow Past an Airfoil. *AIAA J.* **35**(7), 1134-1142.

[28]Craft, T.J., Launder, B.E. and Suga, K. 1995 A Non-linear Eddy-viscosity Model Including Sensitivity to Stress Anisotropy. In *Proc. 10th Symposium on Turbulent and Shear Flows*, pp. 23-19:23-24.

[29]Barakos, G. and Drikakis, D. 2000 Investigation of Non-linear Eddy-viscosity Turbulence Models in Shock-boundary Layer Interaction. *AIAA J.* **38**(3), 461-469.

[30]Sofialidis, D. and Prinos, P. 1997 Development of a Non-Linear Strain-Sensitive $k-\omega$ Turbulence Model. *Proc. 11th Symposium on Turbulent Shear Flows*, 2-89–2-94.

[31]Spalart, P. R. and Allmaras, S. R. 1992 A One-equation Turbulence Model for Aerodynamic Flows. *AIAA Paper 92-0439*.

[32]Wilcox, D. C. 1994 Turbulence Modeling for CFD *DCW Industries, Inc., La Canada, California*.

[33]Menter, F. R. 1993 Zonal Two Equation Kappa-Omega Turbulence Models for Aerodynamic Flows. *AIAA Paper 93-2906*.